



Islamic Azad University



Study of Optical Properties, Thermal Kinetic Decomposition and Stability of Coated PETN-Litholrubine nano-Composite via Solvent/None-Solvent Method Using Taguchi Experimental Design

Masoomeh Saberi Lamraski¹, Saeed Babae^{*1}, Seyed Mahdi Pourmortazavi¹

¹ Faculty of Chemistry and Chemical Engineering, Malek Ashtar University of Technology, Iran.

(Received 13 Sep. 2019; Revised 19 Oct. 2019; Accepted 20 Nov. 2019; Published 15 Dec. 2019)

Abstract: In this research, in order to coating PETN particles, nano-pigment of red litholrubine B 57:1 (NLR) was used in a surfactant environment of cetyltrimethyl ammonium bromide (CTAB) using solvent/none-solvent (water-acetone) method. After structural studies of PETN-NLR nanocomposite by infrared (FT-IR) and field emission scanning electron microscopy-Energy dispersive X-ray (FESEM-EDX) methods, Taguchi statistical design method was used to investigation and optimization of light reflectance of nanocomposite at 532 nm. The effect of four factors of NLR concentration, solvent flow rate, surfactant type and surfactant concentration in three levels on light reflection was investigated and analysis of variance (ANOVA) showed that NLR concentration with the participation of 67.24 percent had highest effect. Optimal conditions to achieve a minimum light reflectance were obtained of NLR 5 wt%, solvent flow rate 1 mLmin⁻¹, surfactant of CTAB and surfactant concentration 1×10⁻³molLit⁻¹. The lowest light reflectance by analyzing the data variance for optimum conditions was estimated 4.67 ± 2.14%. Also the mean experimental result for light reflectance of the nanocomposite under optimum conditions was obtained 5.54 percent. Follows, thermal behavior and vacuum stability of the optimal sample was investigated that the results, due to the no significance difference in the melting point and the thermal decomposition mechanism of the nanocomposite compared to pure PETN, indicating the compatibility of NLR and CTAB with PETN.

Keywords: Optical Properties, Coating, PETN, Thermal Kinetic Decomposition, Solvent-non solvent, Taguchi Statistical Design.

1. INTRODUCTION

The absorption or reflection of various compounds due to the use of light energy in recent decades has been attractive and has significantly extended in basic sciences and various industrial technologies [1-5]. In this regard, many

* Corresponding author. Email: Safnba@gmail.com

studies have also been reported on the interaction of high-energy materials with light waves, especially for improving of the production, safety and transportation process.

Some research has been carried out on propellant and pyrotechnic materials [6-8], and numerous studies have been reported on nitrate esters and nitro amine compounds [9-11]. The use of light rays in combustion of high-energy materials is more safe, environmentally friendly, than conventional methods, such as electrical and mechanical combustion with toxic chemical compounds [11].

When light beam incidence on the surface of an object, a fraction of the light energy is absorbed on its surface. The amount of the absorbed energy is related to the optical, physical and thermal properties of the substance [12]. Combustion of energetic materials is widely used in various applications, such as air bags in vehicles or aircraft launch systems. The mechanism of ignition, is hot spots formation that is related to the stimulating reactions due to the thermal heterogeneities in the matter [13].

According to many researches, the flammability of energetic materials has a thermal phenomena by light waves, and light radiation acts as a heat source for the absorbed matter and so the hot spots start the thermal decomposition reactions [14].

The molecular structure of energetic compounds for light ignition should be absorbing light waves easily from an optical source. If the absorption properties of these compounds are not suitable, these properties should be modified using light absorbents such as magnesium, zirconium or carbon particles. It has been observed that by increasing these powders, the threshold energy of the energetic targets will be reduced to start the ignition [9]. One of the methods for light sensitization for energetic materials is their coating by a secondary compound contain light absorbing groups such as metal nanoparticles [11, 15, 16], organic pigments [17], carbon nanotubes [18, 19] and graphene oxide [20]. In this manner organic pigments are preferred because of their high light absorptions and chemical compatibilities with high-energy materials.

In recent years, coating pretreatments such as microencapsulation [21], emulsion solvent evaporation [22], crystallization [23], spray drying [24] and solvent-non solvent (SNS) [20, 25, 26] methods were used widely to coating of explosives compounds. SNS techniques because of its easy carrying out, single pot process, lower cost, high efficiency and simple equipment is preferable from the others methods.

Among the factors affecting to the coating efficiency of SNS process, the solvent nature, weight ratio of the coating agent to the explosive, time of non-solvent addition and the mixing rate are more important. With proper change of the each factors, a composite with special properties will be produced that can be used for a particular purpose [20].

One of the many ways to optimizing of the main factors is the Taguchi method [27]. It can identify and organize system interactions within experimental data for an analysis lead to an optimal design [28, 29]. Moreover, it is proven that this method can be capable to solve a variety of problems including continuous, discrete and qualitative design variables [30, 31]

Taguchi method classifies the factors as controllable factors and noise factors. Noise factors are variables that influence on the response of a process but cannot be controlled economically. They are not maintained at particular levels during the process period for the expected performance and due to their control difficulties cannot be considered [32, 33].

In this research, Lithol Rubin B nanopigment (NLR) was coated on the surface of pentaerythritol tetranitrate (PETN) powder by solvent-non solvent method in a media contains cetyltrimethyl ammonium bromide (CTAB) via Taguchi statistical design (orthogonal array, 3^4) method. In this regard, the nanocomposite light reflections were evaluated by different factors of NLR mass fraction, solvent flow rate, surfactant type and surfactant concentration.

2. EXPERIMENTAL

2.1. CHEMICAL

High pure PETN was prepared by defense industry (Iran). Lithol Rubin B nanopigment (NLR) was obtained from Main Chem. (Fujian, China) with a particle size range of 20-40 nanometers. The surfactants of sodium dodecyl sulphate (SDS), TritonX-114 (TX114) and N-cetyl-trimethyl ammonium bromide (CTAB) purchased from Across (NewJersey, USA). Ultra-pure water was obtained by a Millipore system (Bedford, England) and the other chemicals were provided from Merck (Darmstadt, Germany).

2.2. EQUIPMENTS

Fourier transform infrared spectrometer (FT-IR) spectra were obtained with a Nicolette 800. *A field emission scanning electron microscopy-Energy dispersive X-ray (Mira3Tscan) was used for morphology and elemental analysis.* PerkinElmer-Lambda-950 has been used to light reflection measurements in 400-1100 nm. Thermal studies were achieved by Netzsch-DSC14 applying heating rate of $5\text{ }^{\circ}\text{Cmin}^{-1}$ under nitrogen atmosphere. Chemical compatibility measurements were carried out using a vacuum stability test according to STANAG4556 standard. All data handling of Taguchi method was performed by using MiniTab-17 software.

2.3. PROCEDURE

Inside a 200 ml backer containing 100 ml of aqueous surfactant, a specific weight of NLR (according to Tab. 1), was added to the backer and the mixture

was subjected to ultrasonic waves (100 Watts) at 40°C for 30 minutes. The PETN solution in acetone was then added drop wise to the mixture meanwhile stirring at 60 °C. After ca. 80% solvent was evaporated, the remaining solution was filtrated. The precipitate was washed 3 times with 5 mL of water and 2 times with ethanol. The precipitant was dried at 60 °C for 24 hours and then its light reflection was measured. Due to the efficient coating of PETN powder by NLR particles, parameters of the coating process were optimized by using of Taguchi statistical method. This experimental design based on OA₉ (3⁴) was performed by changing of four variables (i.e., NLR mass fraction, solvent flow rate, surfactant type and surfactant concentration) at 3 levels that was summarized in Table I.

Table I. Arrangement for the factors and levels of the experiments (OA₉ matrix)

Trial no.	NLR mass fraction (Wt %)	Solvent flow rate (mLmin ⁻¹)	Surfactant type	Surfactant Concentration (molLit ⁻¹)
1	1	1	SDS	1.0× 10 ⁻³
2	1	2	TX114	2.0× 10 ⁻³
3	1	3	CTAB	4.0× 10 ⁻³
4	3	1	TX114	4.0× 10 ⁻³
5	3	2	CTAB	1.0× 10 ⁻³
6	3	3	SDS	2.0× 10 ⁻³
7	5	1	CTAB	2.0× 10 ⁻³
8	5	2	SDS	4.0× 10 ⁻³
9	5	3	TX114	1.0× 10 ⁻³

3. RESULTS AND DISCUSSION

3.1. FT-IR SPECTROSCOPY

Infrared spectroscopy was used to the composition investigation of the produced nanocomposite. Fig. 1 shows the FT-IR spectrum of the PETN, CTAB, NLR and the synthesized nanocomposite samples. In Fig. 1-a, related to PETN spectrum, main absorption peaks are occurred at 2932, 1646, 1269, 1000 and 851cm⁻¹, which are corresponding to the stretching vibrations of CH₂, NO₂(symmetry), NO₂ (asymmetry), CO and NO groups respectively. CTAB spectrum (Fig. 1-b) has a three strong absorption peak of symmetric and asymmetric stretching vibration for CH₂ groups at 2847, 2918 &3012 cm⁻¹. Peaks at 1350-1800 cm⁻¹ related to stretching vibration for CN and CH₂ groups. Also the stretching vibrations of quaternary amine [RN(CH₃)₃⁺]is observed at 600-1000 cm⁻¹. NLR spectrum (Fig. 2-c) has a broad absorption peak of stretching vibration for hydroxyl groups at 3168-3658 cm⁻¹. As shown in Fig. 1-d, related to the nanocomposite spectrum, the CTAB and NLR peaks are seen along with the PETN. Also the appearance abroad peak at 3270-3560 cm⁻¹ is

related to hydroxyl groups of NLR. Thus, the interaction of CTAB and NLR compounds with PETN in nanocomposites is confirmed.

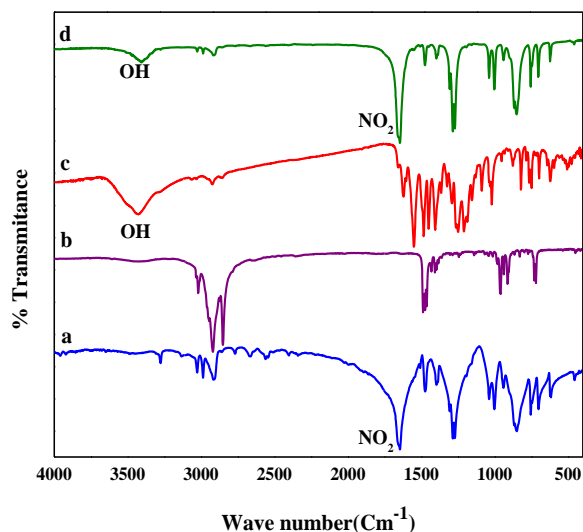


Fig. 1. FT-IR spectra of: (a) PETN; (b) CTAB; (c) NLR and (d) PETN/NLR/CTAB nanocomposite.

3.2. MORPHOLOGICAL-ELEMENTAL ANALYSIS

The morphology, and elemental analysis of PETN, NLR and the synthesized nanocomposite were analyzed via FESEM-EDX system. The results are shown in Fig. 2 (a, b and c) respectively. Fig. 2a-1 relate to FESEM image of pure PETN. As seen PETN crystal has complex tetragonal shaped with relatively smooth surfaces and sharp edges. EDX analysis (Fig. 2a-2) of PETN shows its composition contains carbon, nitrogen and oxygen. FESEM image of NLR is brought in Fig. 2b-1. It shows amorphous particles with a size range of 20-40nm. Elemental analysis of NLR is seen in Fig. 2b-2. FESEM-EDX analysis of the prepared nanocomposite are shown in Fig. 2c-1,2. FESEM image indicates that NLR particles completely cover the surface of the PETN, and the sharpness of the edges, compared to the pure crystals, is lost and a core-shell structure is formed. According to Fig. 2c-2, the results of elemental analysis at the nanocomposite surface indicate that the content of carbon, nitrogen and oxygen is in agreement with the NLR pigment. This result shows that the NLR completely covers the surface of the PETN.

NLR contains hydroxyl groups, and the interaction between these groups with nitro groups in the structure of the PETN causes hydrogen bonding between the hydroxyl group and the oxygen of the nitro group and thus enhances the coating of NLR on the surface of the PETN.

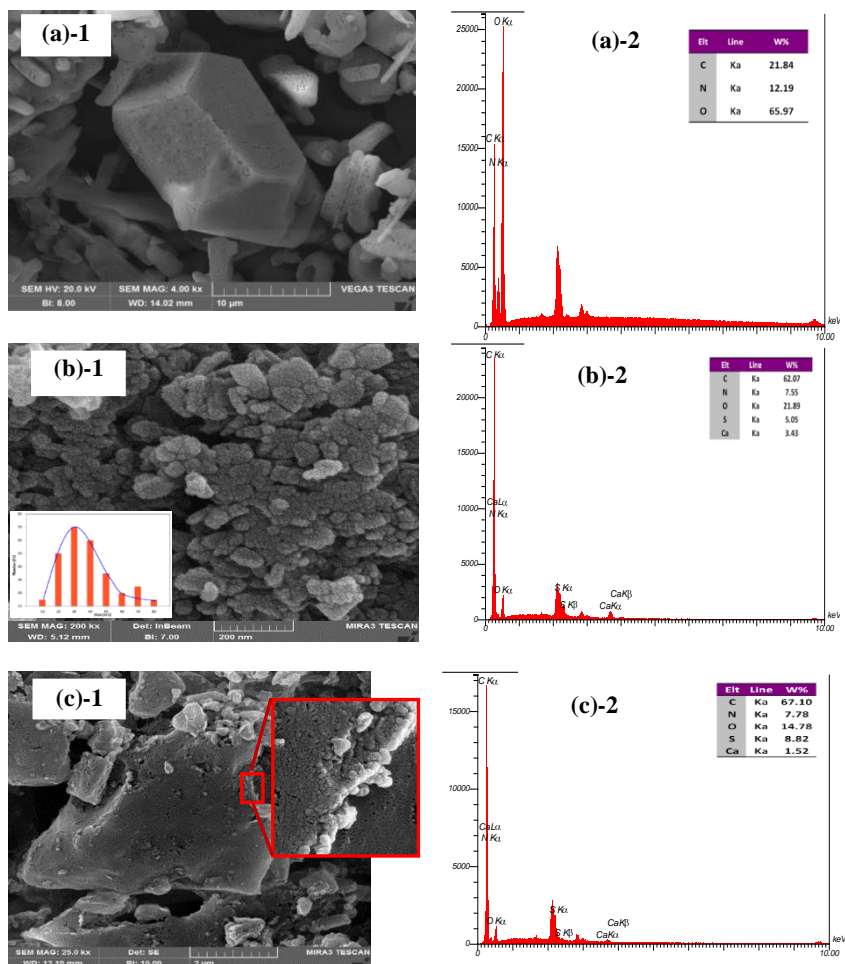


Fig. 2. FESEM- EDX of (a) PETN, (b) NLR and (c) synthesized nanocomposite.

3.3. OPTICAL REFLECTION SPECTROSCOPY

The reflection spectra of the nanocomposites were obtained using circular surfaces with 30 mm diameter in a wavelength range of 400 - 1100 nm. The optical properties of nanocomposites were achieved by spectrometer reflective mode and at deviation angle of 8 degrees with a 2 nm interval.

The Kubelka-Munk equation (Eq. 1) is used to determine the light absorption. This equation expresses the relationship between absorption, emission and reflection of radiation. In this equation, K is the absorption coefficient, S is the emission coefficient and R is the reflection intensity.

$$\frac{K}{S} = \frac{(1 - R)^2}{2R} \quad (1)$$

In accordance with the conditions listed in Table I, the reflection spectra of the synthesized nanocomposites are shown in Fig. 3 Also the reflectance (%) of the specimens at 532 nm was measured and the results are presented in Table II.

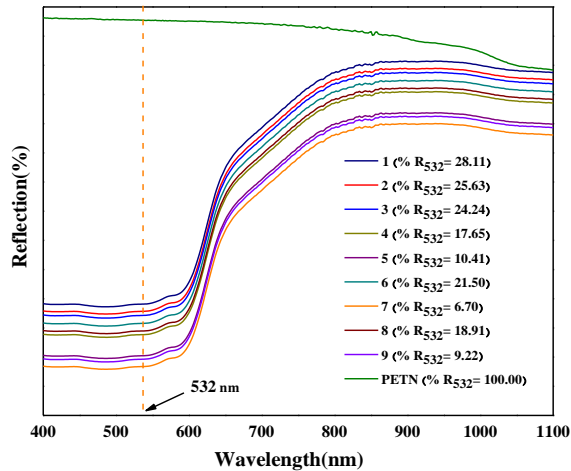


Fig. 3. Reflectance Spectra of PETN-NLR nanocomposites.

Common optimization procedures for stabilizing a multistage process are sequential and simultaneous methods [34, 35]. In sequential methods (one each time optimization), there are some difficulties with them such as slow convergence and too many experiments [36]. In simultaneous optimization methods such as mixture designs [37] and factorial designs [38], the mentioned problems not exists and the optimum conditions would be determined with constructing a response surface or by an extrapolated graph. A clear defect of the factorial designs is that when number of variables increases, the number of the required experimental trials increases geometrically. Therefore, the implement of these trials is not feasible and fast. This problem can be decreased by using of fractional factorial experiments, such as Plackett-Burman schemes or orthogonal array designs (OAD). In comparison to previous two-level designs, OAD has three-level designs and more precise information could be resulted.

In designing experiments, Taguchi applied OAD, which represent the least fractional factorials and is used for the most experiment designs (Eq. 2). The number of possible designs, N , in a full factorial design is as followed:

$$N = L^m \quad (2)$$

Where L is number of levels for each factor and m = number of factors. Thus, if the qualities of a given product depend on four factors and each factor is to be tested at three levels, a full factorial experiment would require 3^4 (81). This

array identified by the symbol L_9 (OA_9) and is used to design experiments involving up to four three-level factors [39, 40].

In this research, four factors (NLR mass fraction, solvent flow rate, surfactant type and surfactant concentration) at three levels were considered and Taguchi method based on OA_9 , with 9 experiments, was applied for the reflection studies of the prepared nanocomposites. The practical results Reflection values (%) are summarized in Table II. As shown, the maximum and minimum reflectances were resulted in experiments no. 2 and no. 7, respectively.

Table II. Result of the reflective test of NLR-PETN nanocomposites.

Trial no.	1	2	3	4	5	6	7	8	9	PETN
Reflection in 532 nm (%)	28.1	25.6	24.2	17.6	10.4	21.5	6.7	18.9	9.2	100.0
	1	3	4	5	1	0	0	1	2	0

Since the maximum light absorption or minimum reflection in the sample is considered, the mean values and the effect for the applied factors (along with the mean of means) on the reflection was calculated using Minitab software and are given in Fig. 4 a-d. It reveals how the reflection of the optimal nanocomposite will change when each level of the factor is altered.

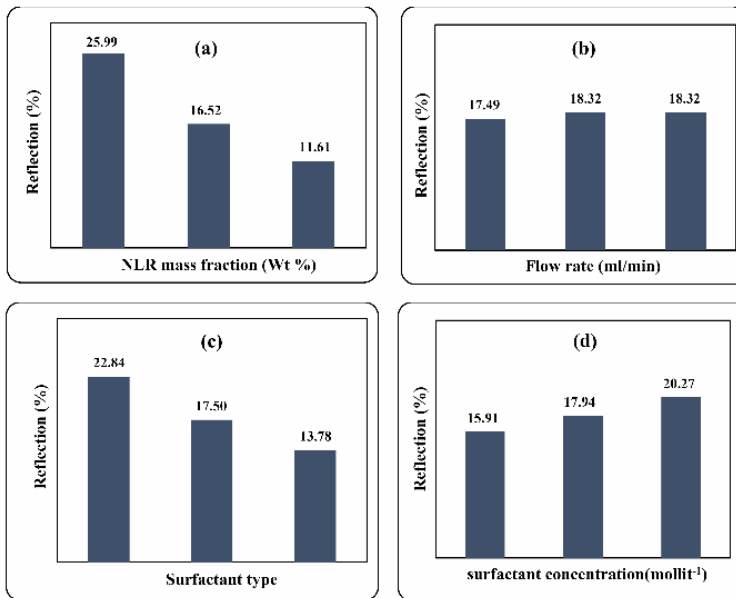


Fig. 4. Effect of optimization parameters along with the mean of means on light reflection (%). (a): NLR mass fraction, (b): solvent flow rate, (c): Surfactant type, (d): Surfactant concentration.

As shown in Figure (4-a), the increase in NLR amounts increase the absorbance intensity at 532 nm significantly, resulting in a much decrease the reflectance. By increasing the amount of NLR to 5% by weight, increases the interaction of NLR hydroxyl group with nitro groups on the surface of the PETN and ultimately, due to the higher coating of NLR on the PETN, decreases the reflection.

Regarding to Fig. 4-b, it seems that the solvent flow rate after 1mLmin^{-1} has a small effect on the nanocomposite reflectance. In general, decreasing the solvent flow rate results to the formation of larger crystals of PETN and so interaction between NLR hydroxyl groups with nitro groups on the PETN surface will be increased. This effect ultimately improves the coating process on the PETN.

Effect of surfactant types on the reflectance of the coated PETN was studied with SDS, CTAB and CTAB. The analysis of Taguchi results in Fig. 4-c show that CTAB has the best influence on the light reflection. CTAB is a surfactant that contains amine groups with positive charge in its structure. Cationic CTAB groups in the vessel media interact with anionic groups on the NLR surface and provide better dispersion along with good stability of the pigment in the solution. As a result better interaction has been occurred for NLR with PETN, and due to the full coating of the surface, the amount of light reflectance has decreased. This effect is not seen by using of anionic SDS and nonionic TX114.

Fig. 5-d shows that by using surfactant concentration of $1 \times 10^{-3} \text{ molLit}^{-1}$, the reflection quantity of the synthesized nanocomposite was decreased. By increasing the concentration of CTAB, the surfactant monomers progress to micelle formation and so ideal dispersion and good stability of NLR in the solution, due to its agglomeration, has not been well done. Therefore the coating yield and following it the amount of light reflection was reduced.

Analysis of variance (ANOVA) was applied to a survey statistical or quantitative evaluation of effects of each factor on reflection. According to the numerical values of F ratio, value of solvent flow rate is less than its F critical value (at 90 % confidence level) and, thus this factor must be pooled [41]. Table III was obtained after pooling the data for one time. According to the results, NLR mass fraction with participation of 67.24 percent has the highest influence on the reflection. With respect to the data, the main factors show that the optimum conditions proposed are sequentially as: NLR mass fraction= 5 wt%, Solvent flow rate = 1.0mLmin^{-1} , Surfactant type= CTAB, Surfactant concentration= $1.0 \times 10^{-3} \text{ molLit}^{-1}$.

Table III. ANOVA results for the Light reflection of Nanocomposite by an OA₉ matrix with H₅₀ as the response (cm)

Factor	Code	DOF	S	V	Pooled ^a			
					DO	S'	F'	P'
NLR mass fraction (Wt)	A	2	320.7	160.3	2	319.3	231.8	67.24
Solvent flow rate	B	2	1.383	0.692	-	-	-	-
Surfactant type	C	2	124.3	62.17	2	122.9	89.89	25.89
Surfactant concentration	D	2	28.47	14.23	2	27.08	20.58	5.70
Error		0	-	-	2	1.383	-	1.17

DOF: degree of freedom, S: standard deviation, V: variance, S': standard deviation after pooling, F': calculated value for the F test; P': participation of each factor on the result after pooling.

^aThe critical value was at 90% confidence level; pooled error results from pooling insignificant effect.

As a general rule, the optimum performance (here, for light reflection test with highest H₅₀) could be calculated by Eq. (3):

$$Y_{opt} = \frac{T}{N} + \left(A_3 - \frac{T}{N}\right) + \left(B_1 - \frac{T}{N}\right) + \left(C_2 - \frac{T}{N}\right) + \left(D_2 - \frac{T}{N}\right) \quad (3)$$

Where Y_{opt} (reflection at the optimum conditions) is equal to the T/N (ratio of the grand total of all results to the total number of all experiments) plus the contributions of A₃ (NLR mass fraction at level 3, 5wt%), B₁ (Solvent flow rate at level 1, 1.0 mLmin⁻¹), C₂ (Surfactant type at level 2, CTAB) and D₂ (Surfactant concentration at level 1, 1.0×10⁻³ molLit⁻¹). The procedure for computation the confidence interval (CI) of the optimum performance is explained following by Eq. (4).

$$CI = \pm \sqrt{\frac{F_{\alpha}(f_1, f_2)V_e}{n_e}} \quad (4)$$

Where, F_α(f₁, f₂) is the critical value for F at degrees of freedom (DOF) f₁ and f₂ at the significance confidence level (In this work α= 90%) f₁ is DOF of the mean (which always equals to 1), f₂= DOF of the error term, V_e is the variance of error term (from ANOVA), n_e is defined as effective number of replications, and expressed by n_e = number of trials/(f₁ + DOF of all factors applied in the estimation of optimum results). Statistical calculations for prediction the result and CI at optimum conditions revealed that the reflection of the nanocomposite will be 4.67± 2.14%.

Due to validation of the optimal conditions obtained by Taguchi method, the light reflection test was applied for the optimum nanocomposite. The reflection

for optimum nanocomposite is equal to 5.54%. This result is in the range of formerly confidence interval and so it is acceptable for this work.

3.4. THERMAL ANALYSIS STUDIES

The thermal performance of high-energy materials is considered as a key property and it affects the preparation process, storage and transportation. Therefore, the study of thermal behavior (including stability, sensitivity and energy content) and thermo-decomposition mechanism of PETN or its nanocomposite is essential [42, 43]. The thermal stabilities of pure PETN and the optimal nanocomposite investigated by differential scanning calorimetric analysis (DSC) and the thermograms were shown in Fig. 5.

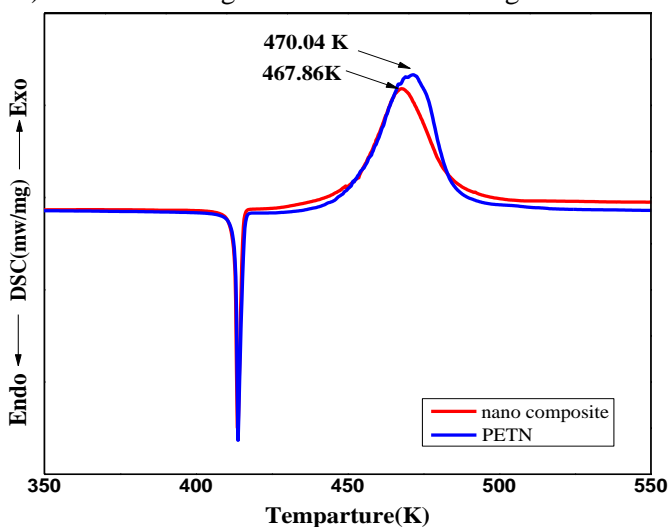


Fig. 5. DSC thermograms of pure PETN (a) and the synthesized nanocomposite (b)

As shown in Fig. 5, two peaks are observed for DSC curves of PETN and the prepared nanocomposite. The first sharp endothermic peaks in 414-415 K which correspond to their melting points and the second are broad exothermic peaks in range of 467-471 K that relate to thermal decomposition of pure PETN [44]. So no significant changes were observed on the melting and decomposition temperatures of the synthesized nanocomposite compared to pure PETN and therefore this negligible difference indicated to thermal adaptability of NLR and CTAB with PETN.

To determine the thermal decomposition kinetic parameters of PETN and the nanocomposite, their DSC behaviors were studied by non-isothermal measurements under different heating rates of 5, 10, 15 and 20 Kmin^{-1} by Kissinger method [43, 45]. As it can be seen in Fig. 6(a-1 and b-1) with increasing of heating rates, the temperature of the exothermic peak increases sequentially. Kissinger's equation is presented by Eq. (5).

$$\ln\left(\frac{T_p^2}{\beta}\right) = \frac{E_a}{RT_p} - \ln\left(\frac{AR}{E_a}\right) \quad (5)$$

Where T_p is the temperature of exothermic peak (K), β is the heating rate (K min⁻¹), E_a is the activation energy (J·mol⁻¹), R is the ideal gas constant (8.314 J·mol⁻¹ K⁻¹) and A is the pre-exponential factor. According to equation (4) when $\ln(T_p^2/\beta)$ values are plotted against $10^3/T_p$ values, a straight line is obtained that E_a and A factors are the slope and intercept of the line respectively. The calculated activation energies of PETN and the nanocomposite were resulted 152.33 kJmol⁻¹ and 146.63 kJmol⁻¹ respectively (Fig.6-a2 and 6-b2). Reduction in the activation energy equal to 5.7 kJmol⁻¹ for nanocomposite, exhibits greater activity than the pure PETN. However the partial change in activation energy between pure PETN and the synthesis nanocomposite showed that the added NLR was not altered the decomposition mechanism of the pure PETN.

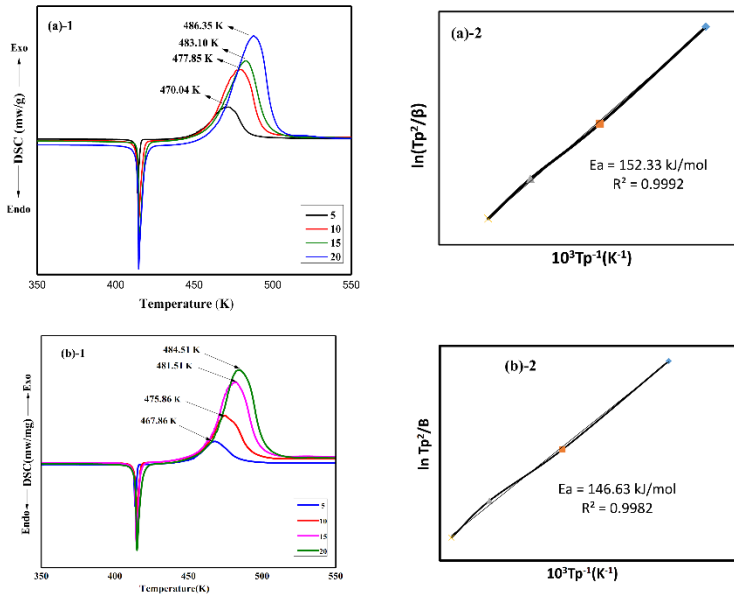


Fig. 6. DSC curves with Kissinger plots of PETN (a-1,2) and nanocomposite (b-1,2).

3.5. VACUUM STABILITY TEST

One of the few ways for measuring chemical compatibility for explosives is vacuum stability test (VST) method. In this technique, the volume of released gas from an energetic compound is measured under a defined temperature at a specific time and then the result compares with the standard value. If the resulting quantity is less than standard value, the examined compound is stable. According to the STANAG4556 standard, required temperature for PETN is 120 °C through 20 hours. The VST results for pure PETN and the prepared

nanocomposite are shown in Tab. 4. The data given indicate to chemical compatibility of NLR and CTAB with PETN.

Table IV. Data Results of vacuum stability test for PETN and the prepared nanocomposite.

Sample	Evolved gas	Standard evolved gas
PETN	0.18	2.0
Optimal	0.28	2.0

4. CONCLUSION

In this research, nanocomposite of PETN\NLR\CTAB was prepared via solvent-non solvent method. FT-IR, FESEM and EDX analysis indicated that PETN particles were coated by NLR along with CTAB. Taguchi design method was considered to optimize experimental conditions of the coating process. In this manner, four factors (NLR mass fraction, solvent flow rate, surfactant type and surfactant concentration) at three levels were considered and light reflection response was used to the experimental design optimization. According to Taguchi method, the optimal composition of the synthesized nanocomposite was obtained as 5 wt% NLR mass fraction (P%=67.24), Surfactant type of CTAB (P%=25.89) and 1.00×10^{-3} molLit⁻¹ CTAB concentration (P%=5.70). The ANOVA analysis showed that the effect of the solvent flow rate was negligible. The light reflection under optimum conditions was predicted by Taguchi design ($4.67 \pm 2.14\%$) and experiment results (5.54%) were in satisfactory agreement. It is mentioned that compared to the pure PETN, with this process the light reflection decreased from 100.0 to 6.7%. To complementary studies, thermal analysis (decomposition kinetics) and vacuum stability test methods showed to thermal adaptability and chemical compatibility of NLR and CTAB with PETN in the produced nanocomposite. The obtained results revealed that this method is a proper process for the PETN coating with the negligible energy reduction.

REFERENCES

- [1] R. Akhmetshin, A. Razin, V. Ovchinnikov, A. Skripin, V. Tsipilev, V. Oleshko, V. Zarko, A. Yakovlev, *Effect of laser radiation wavelength on explosives initiation thresholds*, Journal of Physics: Conference Series, IOP Publishing, (2014) 012015.
- [2] M. Borhani Zarandi, H. Amrollahi Bioki. *Effects of Cobalt Doping on Optical Properties of ZnO Thin Films Deposited by Sol-Gel Spin Coating Technique*. Journal of Optoelectrical Nanostructures. 2(4) (2017) 33-44.
- [3] M. Shirkevand, M. Bavir, A. Fattah, H. R. Alaei, T. Najaran, M. Hossein. *The Construction and Comparison of Dye-Sensitized Solar Cells with*

- Blackberry and N719 Dyes*. Journal of Optoelectrical Nanostructures. 3(1) (2018) 79-92.
- [4] N. Roostaie, E. Sheykhi, F. Japelaghi, M. A. Bassam, S. Tavaddod, B. Sajad. *A Thin Layer Imaging with the Total Internal Reflection Fluorescence Microscopy*. Journal of Optoelectrical Nanostructures. 2(3) (2017) 47-54.
- [5] M. Zoghi. *Reflection Shifts in Gold Nanoparticles*. Journal of Optoelectrical Nanostructures. 3(1) (2018) 1-14.
- [6] D. N. Herreros, X. Fang. *Laser ignition of elastomer-modified cast double-base (EMCDB) propellant using a diode laser*. Optics & Laser Technology. 89 (2017) 21-26.
- [7] H. M. Wang, X. Chen, C. Zhao, NEPE propellant ignition and combustion under laser irradiation, *Advanced Materials Research, Trans Tech Publ*, (2014) 10-14.
- [8] N.-S. Jang, S.-H. Ha, K.-H. Kim, M. H. Cho, S. H. Kim, J.-M. Kim. *Low-power focused-laser-assisted remote ignition of nanoenergetic materials and application to a disposable membrane actuator*. Combustion and Flame. 182 (2017) 58-63.
- [9] X. Fang, W. G. McLuckie. *Laser ignitibility of insensitive secondary explosive 1, 1-diamino-2, 2-dinitroethene (FOX-7)*. Journal of hazardous materials. 285 (2015) 375-382.
- [10] I. Assovskiy, G. Melik-Gaikazov, G. Kuznetsov, Direct laser initiation of open secondary explosives, *Journal of Physics: Conference Series*, IOP Publishing, 2015, 653 012014.
- [11] X. Fang, M. Sharma, C. Stennett, P. P. Gill. *Optical sensitisation of energetic crystals with gold nanoparticles for laser ignition*. Combustion and Flame. 183 (2017) 15-21.
- [12] H. Oestmark, N. Roman. *Laser ignition of pyrotechnic mixtures: Ignition mechanisms*. Journal of applied physics. 73(4) (1993) 1993-2003.
- [13] W. Hawthorne, D. Weddell, H. Hottel. *Third Symposium on Combustion and Flame and Explosion Phenomena*. The Williams and Wilkins Co., Baltimore, Maryland. (1949) 266-288.
- [14] E. D. Aluker, A. G. Krechetov, A. Y. Mitrofanov, A. S. Zverev, M. M. Kuklja. *Understanding limits of the thermal mechanism of laser initiation of energetic materials*. The Journal of Physical Chemistry C. 116(46) (2012) 24482-24486.

- [15] B. Aduiev, D. Nurmukhametov, R. Furega, I. Liskov. *Initiation of Explosion of Pentaerythritol Tetranitrate by Pulses of the First and Second Harmonics of a Neodymium Laser*. Russian Physics Journal. 58(8) (2015).
- [16] I. Y. Zykov. *The critical initiation energy density of PETN with aluminum nanoparticle additives*. Modern fundamental and applied researches. 1(8) (2013) 79-84.
- [17] X. Fang, S. R. Ahmad. *Laser ignition of an optically sensitised secondary explosive by a diode laser*. Central European Journal of Energetic Materials. 13(1) (2016).
- [18] H. Kim, A. Lagutchev, D. D. Dlott. *Surface and interface spectroscopy of high explosives and binders: HMX and Estane*. Propellants, Explosives, Pyrotechnics: An International Journal Dealing with Scientific and Technological Aspects of Energetic Materials. 31(2) (2006) 116-123.
- [19] J. H. Kim, J. Y. Ahn, H. S. Park, S. H. Kim. *Optical ignition of nanoenergetic materials: The role of single-walled carbon nanotubes as potential optical igniters*. Combustion and Flame. 160(4) (2013) 830-834.
- [20] R. Li, J. Wang, J. P. Shen, C. Hua, G. C. Yang. *Preparation and characterization of insensitive HMX/graphene oxide composites*. Propellants, Explosives, Pyrotechnics. 38(6) (2013) 798-804.
- [21] Z. Yang, L. Ding, P. Wu, Y. Liu, F. Nie, F. Huang. *Fabrication of RDX, HMX and CL-20 based microcapsules via in situ polymerization of melamine-formaldehyde resins with reduced sensitivity*. Chemical Engineering Journal. 268 (2015) 60-66.
- [22] Y. Li, Z. Yang, J. Zhang, L. Pan, L. Ding, X. Tian, X. Zheng, F. Gong. *Fabrication and characterization of HMX@ TPEE energetic microspheres with reduced sensitivity and superior toughness properties*. Composites Science and Technology. 142 (2017) 253-263.
- [23] J.-W. Jung, K.-J. Kim. *Effect of supersaturation on the morphology of coated surface in coating by solution crystallization*. Industrial & Engineering Chemistry Research. 50(6) (2011) 3475-3482.
- [24] W. Ji, X. Li, J. Wang, B. Ye, C. Wang. *Preparation and Characterization of the Solid Spherical HMX/F2602 by the Suspension Spray-Drying Method*. Journal of Energetic Materials. 34(4) (2016) 357-367.
- [25] C. W. An, F. S. Li, X. L. Song, Y. Wang, X. D. Guo. *Surface Coating of RDX with a Composite of TNT and an Energetic-Polymer and its Safety Investigation*. Propellants, Explosives, Pyrotechnics: An International

Journal Dealing with Scientific and Technological Aspects of Energetic Materials. 34(5) (2009) 400-405.

- [26] C. An, J. Wang, W. Xu, F. Li. *Preparation and properties of HMX coated with a composite of TNT/energetic material*. Propellants, Explosives, Pyrotechnics. 35(4) (2010) 365-372.
- [27] T.-H. Hou, C.-H. Su, W.-L. Liu. *Parameters optimization of a nano-particle wet milling process using the Taguchi method, response surface method and genetic algorithm*. Powder Technology. 173(3) (2007) 153-162.
- [28] S. Babae, Z. Monjezi, M. S. Tagharoodi. *Preparation of epoxy-based insulator and optimization of its thermal property by Taguchi robust design method in double base propellant grain application*. Iranian Polymer Journal. 26(3) (2017) 213-220.
- [29] S. M. Pourmortazavi, S. Babae, F. S. Ashtiani. *Statistical optimization of microencapsulation process for coating of magnesium particles with Viton polymer*. Applied Surface Science. 349 (2015) 817-825.
- [30] S. Yim. *Selection of Actuator Combination in Integrated Chassis Control Using Taguchi Method*. International Journal of Automotive Technology. 19(2) (2018) 263-270.
- [31] Z. Khaghanpour, S. Naghibi. *Application of the Taguchi approach to optimize ZnO synthesis via hydrothermally assisted sol-gel method*. Turkish Journal of Chemistry. 42(2) (2018).
- [32] C.-C. Yang, S.-T. Wang. *Improvement of Mechanical Properties of Spheroidized 10B21 Steel Coil Using Taguchi Method of Robust Design*. Sensors and Materials. 30(3) (2018) 503-514.
- [33] E. Olakanmi. *Optimization of the quality characteristics of laser-assisted cold-sprayed (LACS) aluminum coatings with Taguchi design of experiments (DOE)*. Materials and Manufacturing Processes. 31(11) (2016) 1490-1499.
- [34] C. Carino. *Structural layout assessment by orthogonal array based simulation*. Mechanics Research Communications. 33(3) (2006) 292-301.
- [35] M. Mahmoodian, A. B. Arya, B. Pourabbas. *Synthesis of organic-inorganic hybrid compounds based on Bis-GMA and its sol-gel behavior analysis using Taguchi method*. dental materials. 24(4) (2008) 514-521.
- [36] K. Bouacha, M. A. Yaltese, T. Mabrouki, J.-F. Rigal. *Statistical analysis of surface roughness and cutting forces using response surface methodology*

- in hard turning of AISI 52100 bearing steel with CBN tool. International Journal of Refractory Metals and Hard Materials.* 28(3) (2010) 349-361.
- [37] D.-J. Lee, J.-H. Park, M.-C. Kang. *Optimization of TiC Content during Fabrication and Mechanical Properties of Ni-Ti-Al/TiC Composites Using Mixture Designs.* Materials. 11(7) (2018) 1133.
- [38] A. F. Neto, A. F. B. Costa, M. F. de Lima. *Use of Factorial Designs and the Response Surface Methodology to Optimize a Heat Staking Process.* Experimental Techniques. 42(3) (2018) 319-331.
- [39] R. K. Roy, A primer on the Taguchi method, Society of Manufacturing Engineers 2010.
- [40] S. Hosseini, S. Pourmortazavi, M. Fathollahi. *Orthogonal array design for the optimization of silver recovery from waste photographic paper.* Separation science and technology. 39(8) (2005) 1953-1966.
- [41] N. Kang, J. Kim, Y. Park. *Integration of marketing domain and R&D domain in NPD design process.* Industrial Management & Data Systems. 107(6) (2007) 780-801.
- [42] J.-S. Lee, C.-K. Hsu, C.-L. Chang. *A study on the thermal decomposition behaviors of PETN, RDX, HNS and HMX.* Thermochemica Acta. 392 (2002) 173-176.
- [43] K.-S. Jaw, J.-S. Lee. *Thermal behaviors of PETN base polymer bonded explosives.* Journal of thermal analysis and calorimetry. 93(3) (2008) 953-957.
- [44] H. R. Pouretdal, S. Damiri, M. Ravanbod, M. Haghdoost, S. Masoudi. *The kinetic of thermal decomposition of PETN, Pentastite and Pentolite by TG/DTA non-isothermal methods.* Journal of Thermal Analysis and Calorimetry. 129(1) (2017) 521-529.
- [45] M. Künzel, Q.-L. Yan, J. Šelešovský, S. Zeman, R. Matyáš. *Thermal behavior and decomposition kinetics of ETN and its mixtures with PETN and RDX.* Journal of Thermal Analysis and Calorimetry. 115(1) (2014) 289-299.

